SUPPORTING INFORMATION

SEQUENCE-PROGRAMMABLE MULTI-COMPONENT MULTILAYERS OF NANOMETER-SIZED TETRALACTAM MACROCYCLES ON GOLD SURFACES

Sebastian Richter,[a] Christoph H.-H. Traulsen,[a] Thomas Heinrich,[a,b] Johannes Poppenberg,[a] Charlene Leppich,[a] Markus Holzweber, [b] Wolfgang E. S. Unger*[b] and Christoph A. Schalley*[a]

[a] Institut für Chemie und Biochemie, Freie Universität Berlin, Takustraße 3, 14195 Berlin, Germany
[b] BAM, Bundesanstalt für Materialforschung und -prüfung, Unter den Eichen 44-46, 12203 Berlin, Germany

Table of Contents:

1. General methods

Synthetic reactions were conducted under a dry argon atmosphere. Chemicals were purchased from Alfa Aesar or Sigma-Aldrich and used without further purification. Dry solvents were purchased from ACROS Organics and used as received. Diethylether (Et_2O), hexane and ethylacetate were purchased from VWR and destilled prior to use by common laboratory methods. Ethanol (EtOH), dichloromethane (DCM), acetonitrile (ACN) and dimethylformamide (DMF) used for SAM preparation and metal or macrocycle deposition experiments were purchased from Carl Roth and VWR in HPLC grade and used as received. Thin-layer chromatography was carried out on precoated silica gel 60/F254 plates (Merck KGaA) and aluminium oxide N/UV254 plates (Macherey-Nagel). Aluminium oxide (neutral; 0.05 - 0.20 mm; ACROS) and silica gel 60M (0.04-0.063 mm, Machery-Nagel) was used for column chromatography. Gold substrates (30 nm thickness) used for XPS and NEXAFS were prepared onto polished single-crystal Si(100) wafers which have been precoated with a 9 nm titanium adhesion layer. Semitransparent Au substrates (20 nm thickness) used for transmission UV/Vis spectroscopy were prepared on borosilicate glass with a 1 nm titanium adhesion layer. All gold substrates were purchased from Georg Albert PVD (Germany) and stored under argon prior to use. All SAM preparations and metal depositions were performed in gamma-sterilized tubes (Orange Scientific).

2. Instrumentation and data processing

NMR spectra were acquired on a Bruker ECX 400 (^{1}H at 400 MHz, ^{13}C at 101.8 MHz) and a Bruker 700 (^{1}H: 700 MHz; ^{13}C: 175 MHz, ^{19}F at 471 MHz) spectrometer at r. t. Exact masses were determined on AGILENT 6210 ESI-TOF and an Ionspec QFT-7 ESI-FTICR mass spectrometer.

XPS measurements were carried out with an AXIS Ultra DLD electron spectrometer manufactured by Kratos Analytical, UK. XP spectra were recorded using monochromatic Al K_α excitation at a pass energy of 40 eV for all detail spectra and 80 eV for the survey spectrum. The source-to-analyzer angle was 60°. Emission angles of 0° and 60° were used. The binding energy scales of XP spectra were analyzed with Unifit 2013 fitting software (Unifit Scientific Software GmbH, Leipzig, Germany) and all peak fits were performed with a Lorentzian-Gaussian sum function peak shape model. The FWHM values in the N 1s and C 1s spectra were constrained to be equal for each component

per spectrum. Peak fits and integrated peak areas were obtained after subtraction of Shirley backgrounds (Au $4f_{7/2}$, C 1s, Fe $2p_{3/2}$, Ni $2p_{3/2}$ and Pd $3d_{5/2}$). In case of N 1s, this approach was not applicable, because that low intensity peak is superimposed by the intense loss structure of the Au 4d photoemission doublet. A requirement for the application of a Shirley-Background is a higher count rate at the upper binding energy limit of the energy window used for background determination, but in the given case (due to superposition of Au 4d), we have a lower count rate at the upper binding energy limit. As a workaround, a linear background was used in this specific case. Of course, by doing this, the uncertainty of measurement will be increased, but stays at an acceptable level.

The layer thickness *d* is estimated by introducing the attenuation of the XPS Au $4f_{7/2}$ signal intensity at an emission angle of $\vartheta = 60°$ in the following equation:[1]

$$d = \lambda(KE) \cdot cos\vartheta \cdot ln\left(\frac{I_0}{I}\right)$$

The measured Au 4 $f_{7/2}$ peak areas for covered surfaces (I) and for Ar^+ ion-sputtered clean gold substrate (I_0) were used for the calculation. The value for the inelastic mean free path $\lambda(KE)$ = 4.1 nm was calculated with an equation developed by Seah et al. for organic compounds.[2]

NEXAFS measurements were carried out at the HESGM CRG dipole magnet beamline at the synchrotron radiation source BESSY II (Berlin, Germany). The spectra were acquired in the PEY (partial electron yield) mode using a channel plate detector with a retarding field of -150 V and incident angles of linearly polarized synchrotron light of 30° (electric field vector upright to surface plane) and 90° (electric field vector parallel to the surface plane).[3] The resolution $E/\Delta E$ of the monochromator at the carbonyl π* resonance (hν = 287.4 eV) was in the order of 2500. Raw spectra were divided by ring current and monochromator transmission function which was obtained with a freshly sputtered Au sample.[3] Energy alignment of the energy scale was achieved by using an I_0 feature referenced to a C1s→ π* resonance measured with a fresh surface of HOPG (highly ordered pyrolytic graphite, Advanced Ceramic Corp., Cleveland, USA) at 285.4 eV.[4] Spectra are shown with the pre-edge count rate subtracted and after normalization in units of the absorption edge jump.[3] C K-edges were measured at 30° (electric field vector parallel to surface plane), 55° and 90° (electric field vector upright to the surface plane) incident angle of the linearly polarized light beam.

All ToF-SIMS measurements were performed without further cleaning of the sample surface on a ToF.SIMS IV instrument (ION-TOF GmbH, Münster, Germany) of the reflectron-type, equipped with a 25 keV bismuth liquid metal ion gun (LMIG) as primary ion source mounted at 45° with respect to the sample surface. The LMIG was operated at 0.5 µA emission current in the so-called "high current bunched" mode (high mass resolution, low lateral resolution). Bi_3^+ was selected as primary ion by appropriate mass filter settings. To improve the focus of the primary ion beam (and hence the lateral resolution) the pulse width of the Bi_3^+ (25 keV) ion pulse was reduced to 11 ns and the lens target was adjusted to obtain a sharp image on a structured sample (e.g. silver cross) in the secondary electron mode. The primary ion current was directly determined at 150 µs cycle time (i.e. a repetition rate of 6.67 kHz) using a Faraday cup located on a grounded sample holder. Operation conditions with these settings comprised a target current of 0.15 - 0.17 pA for the selected primary ion. The total primary ion dose density was set to 5 x 10^{11} ions/cm^2 ensuring static conditions. Scanning area for analysis was 200×200 μm^2 with a pixel resolution of 256x256. The vacuum in the analysis chamber was in the range of 10^{-9} mbar during all measurements.

ToF-SIMS spectra were acquired in positive ion mode with 5 spots per sample analysed. The mass scale was internally calibrated using a number of well-defined and easily assignable secondary ions ($C_3H_2^+$, $C_4H_2^+$ and $C_5H_2^+$) keeping the error in calibration for all spectra below 10 ppm.

3. Preparation and characterization of new compounds

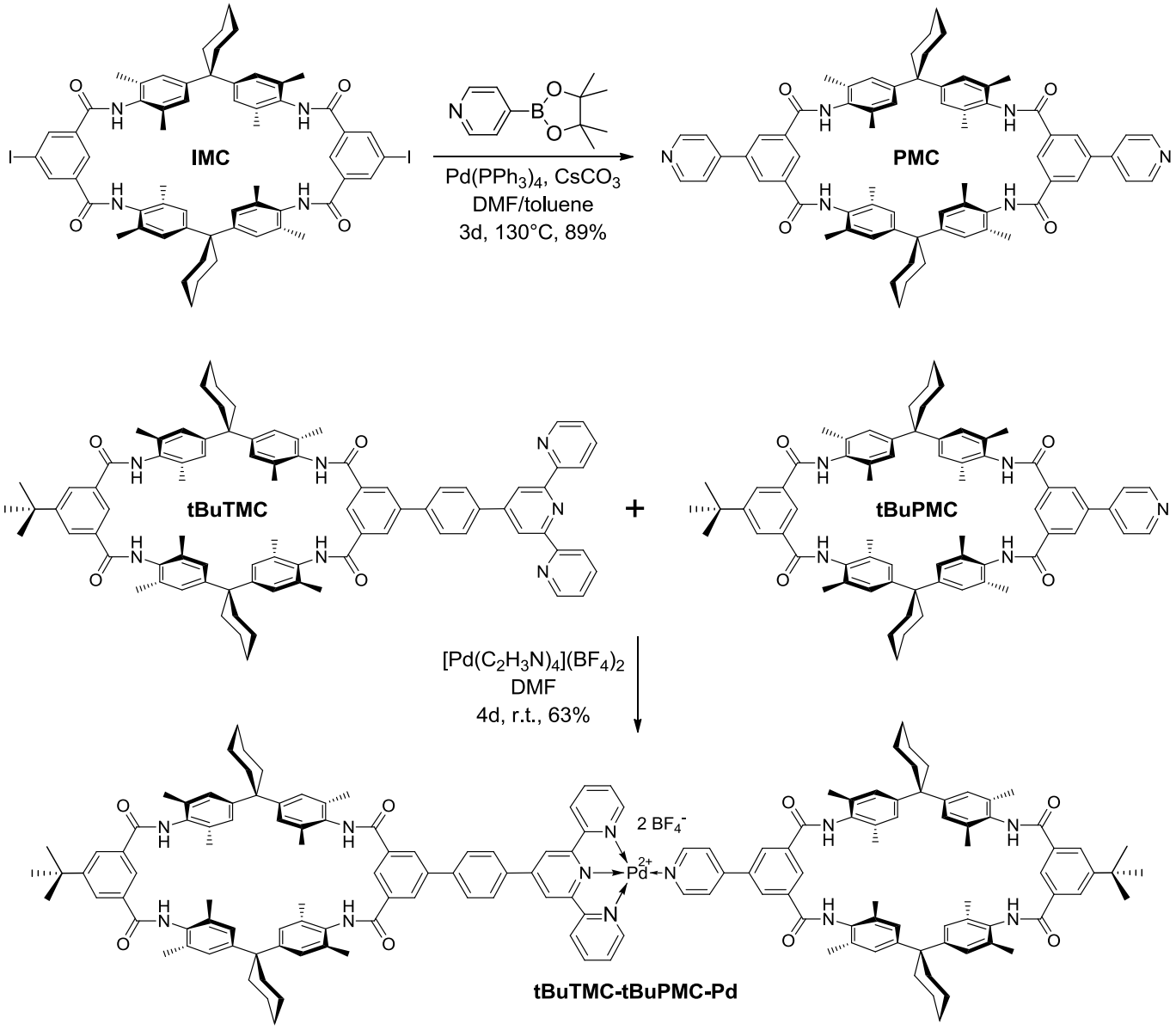

Figure S1. Schematic drawing of the compounds used and new reactions. The macrocycles **TMC**, **IMC**, **tBuTMC**, **tBuPMC** and the test complex **tBuPMC$_2$PdCl$_2$** were prepared as reported.[5-6]

Macrocycle PMC. Diiodo-substituted macrocycle **IMC** (54 mg, 0.047 mmol), cesium carbonate (46 mg, 0.141 mmol) and tetrakis(triphenylphosphine)palladium (6 mg, 0.005 mmol) were dissolved in 25 ml DMF/toluene 1:1. The mixture was heated to 100°C and 4-pyrdineboronic acid pinacol ester (21 mg, 0.1034 mmol) was added, afterwards the temperature was kept at 130°C. After one day, 46 mg cesium carbonate, 6 mg tetrakis(triphenylphosphine)palladium and 21 mg 4-pyrdineboronic acid pinacol ester were added and the reaction mixture was kept at 130°C for 2 days. The solvent was removed under reduced pressure and the crude product was filtered through a thin layer of neutral aluminum oxide (ca. 5 cm in height and 5 cm in diameter) with DMF/toluene 1:1 as the eluent. The filtrate was concentrated *in vacuo* and purified by dialysis (MWCO = 1000, DCM/methanol 4:1, two solvent exchanges) over night and afterwards by preparative TLC (neutral aluminum oxide, DCM/methanol/TEA 50:1:1) affording 44.7 mg (0.042 mmol) of pure product. Yield: 89%; ^{1}H NMR (400 MHz, chloroform-*d*): δ = 8.64 – 8.73 (m, 6H, 2-isophthH and ArH(py)), 8.49 (s, 4H, 4,6-isophthH), 7.64 (d, J = 5.5 Hz, 4H, ArH(py)), 7.02 (s, 8H, ArH), 2.34 (br, 8H, CH_2), 2.18 (s, 24H, $ArCH_3$), 1.62 (br, 8H, CH_2), 1.50 (br, 4H, CH_2) ppm. ^{13}C NMR (176 MHz, chloroform-*d*/DMF-*d7*

10/1): δ = 164.65, 150.11, 147.54, 146.60, 139.30, 135.30, 134.74, 131.61, 129.60, 126.55, 125.75, 121.47, 44.57, 34.77, 26.07, 22.53, 18.62 ppm. HR-MS (ESI, pos. mode, DCM): m/z: calcd. for $[C_{70}H_{71}N_6O_4]^+$: 1059.5531 ($[M+H^+]^+$); found: 1059.5531.

Macrocycle test complex tBuTMC-tBuPMC-Pd. Monoterpyridine-substituted macrocycle tBuTMC (20.3 mg, 0.016 mmol) and tetrakis(acetonitrile)palladium(II)bis(tetrafluoroborate) (7.1 mg, 0.016 mmol) were dissolved in 15 ml dry DMF and stirred at r.t. overnight. Monopyridine-substituted macrocycle **tBuPMC** (16.6 mg, 0.016 mmol) was added and the solution was stirred for 3 days. The mixture was concentrated *in vacuo* to 1-2 ml and 50 ml diethylether were added. The precipitate was centrifuged, the solvent was decanted and the solid was suspended in diethylether. This procedure was repeated three times. Finally, the solvent was decanted, the precipitate transferred into acetonitrile and concentrated *in vacuo* to give **tBuTMC-tBuPMC-Pd** (26.4 mg, 0.01 mmol, 63%) as a yellow solid. ^{1}H NMR (DMF-d_7, 700 MHz): δ = 9.44 (s, 2H, ArH), 9.22 – 9.28 (m, 4H, ArH), 9.00 – 9.05 (m, 2H, ArH), 8.92 (s, 1H, ArH), 8.83 – 8.87 (m, 2H, ArH), 8.67 (s, 2H, ArH), 8.57 – 8.64 (m, 3H, ArH), 8.44 – 8.54 (m, 5H, ArH), 8.13 – 8.22 (m, 7H, ArH), 8.01 (s, 2H, ArH), 7.24 (s, 8H, ArH), 7.22 (s, 8H, ArH), 2.46 (br, 16H, CH_2), 2.21 (s, 24H, $ArCH_3$), 2.17 (s, 24H, $ArCH_3$), 1.62 (br, 16H, CH_2), 1.51 (br, 8H, CH_2), 1.39 (s, 18H, CH_3); Due to the low solubility of **tBuTMC-tBuPMC-Pd**, it was impossible to record a ^{13}C NMR-spectrum; ^{19}F NMR (DMF-*d7*, 376 MHz): δ = -150.55 (s, 8F, BF_4^-) ppm. HR-MS (ESI, pos. mode, DMF/MeOH): m/z: calcd. for $[C_{154}H_{160}N_{12}O_8PdCl]^+$: 2448.1206 ($[M-2BF_4^-+Cl^-]^+$); found: 2448.1135 (δ = 2.9 ppm).

4. Multilayer preparation

Multilayers were prepared on a **PST** pyridine-terminated self-assembled monolayer as template layer described elsewhere.[7] Iron(II) tetrafluoroborate hexahydrate, nickel(II) tetrafluoroborate hexahydrate, tetrakis(acetonitrile)palladium(II)bis(tetrafluoroborate) and bis(benzonitrile)palladium(II) dichloride were used as metal sources. For metal deposition, the samples were immersed in a 1 mM solution of the metal salt in ethanol (iron and nickel salt) or acetonitrile (palladium salts) for 10 min (pyridine-terminated top layer) or 30 min (terpyridine-terminated top layer) at r.t. Deposition of the macrocycles took place by immersing the samples in a 1 mM solution of **TMC** in DMF or **PMC** in DCM for 24 h at r.t. To form the multilayer, both steps were alternatingly repeated until the desired number of layers was reached. To form a programmed multi-component multilayer, different metal and macrocycle solutions were used in the deposition sequence. After each deposition step, the samples were immersed in the corresponding solvent (ethanol, DMF, DCM or acetonitrile) for another 10 min. For characterization, the samples were dried vigorously in a stream of argon and stored under argon before characterization.

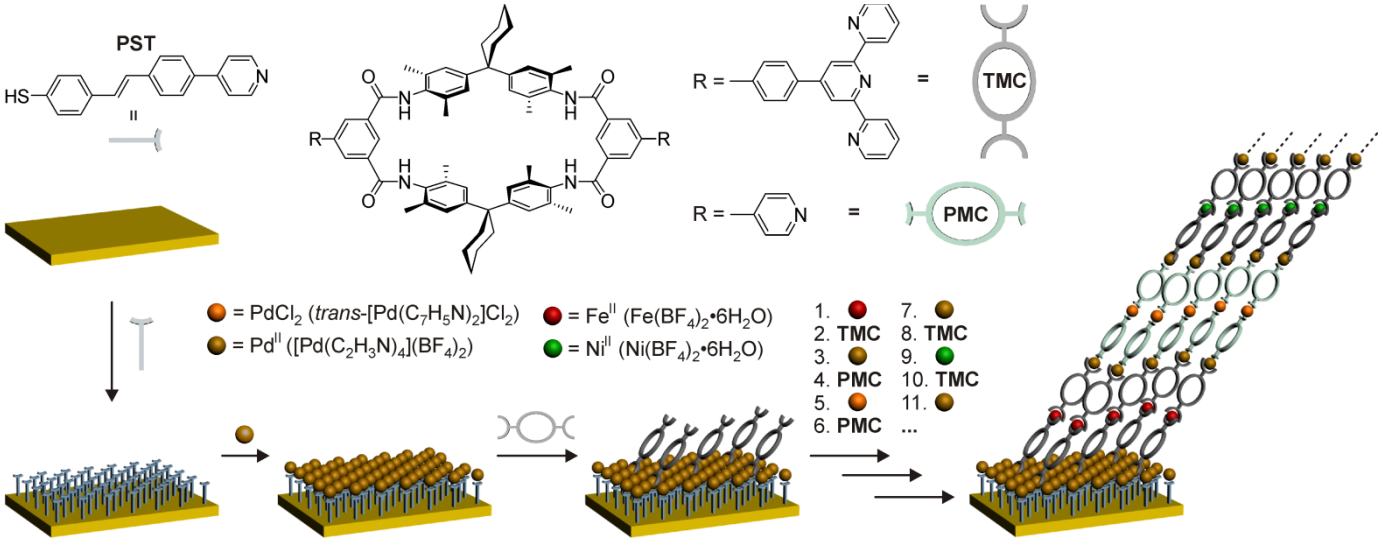

Figure S2. Preparation of the programmed multi-component multilayer as an example for the general multilayer formation.

5. ^{1}H, ^{13}C and ^{19}F NMR Spectra

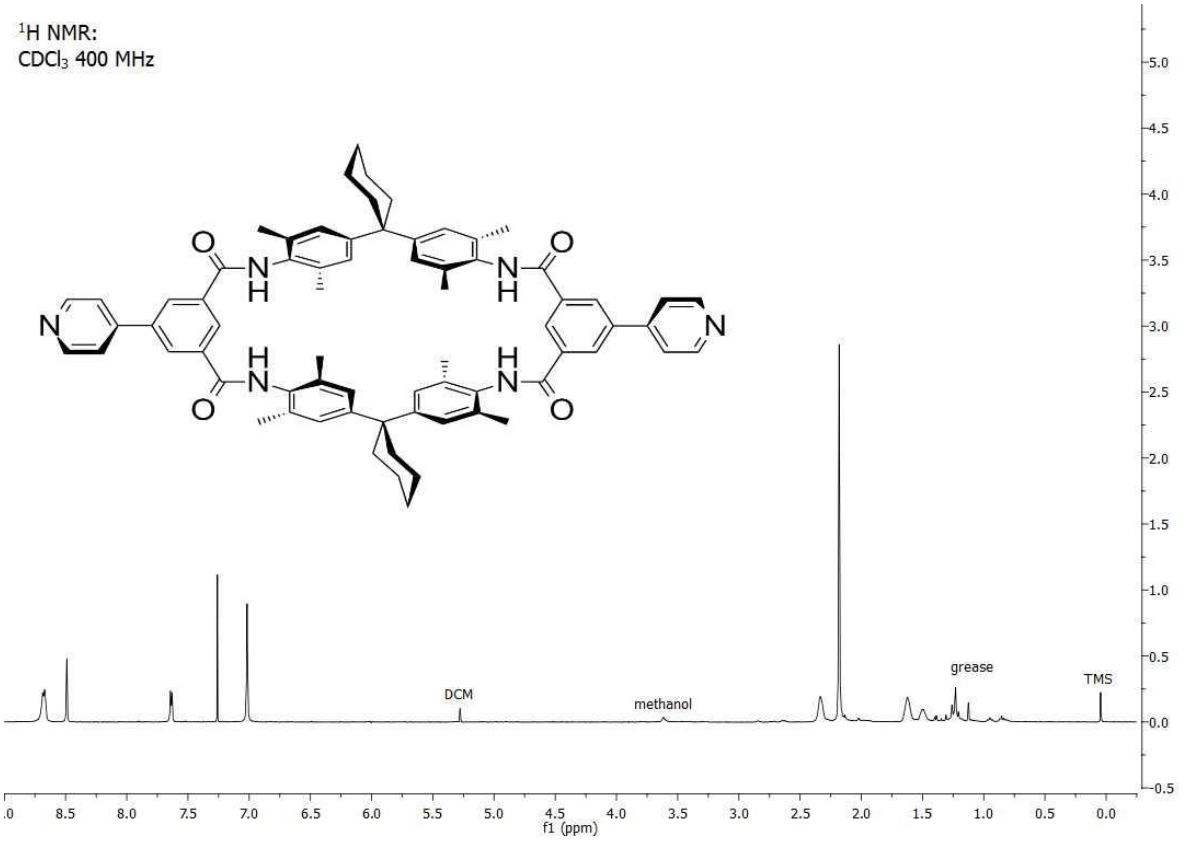

Figure S3: ^{1}H NMR spectrum of **PMC**.

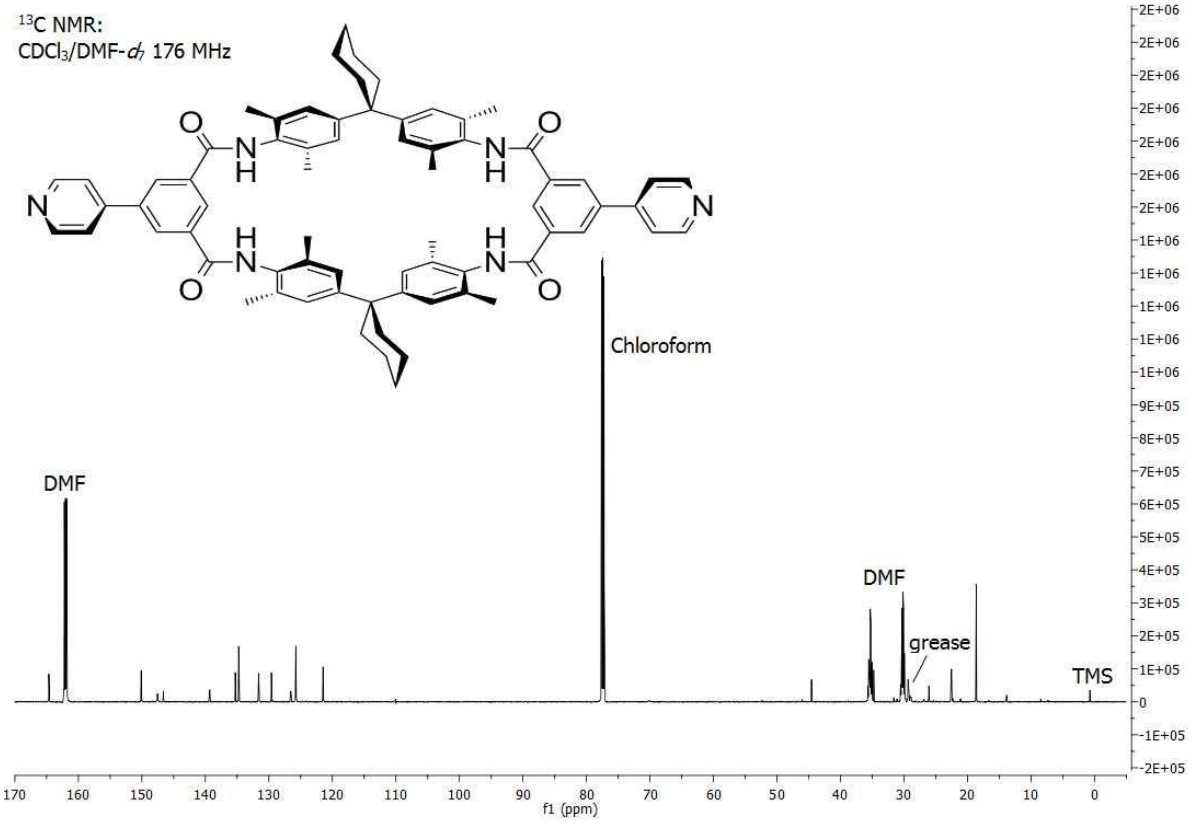

Figure S4: ^{13}C NMR spectrum of **PMC**.

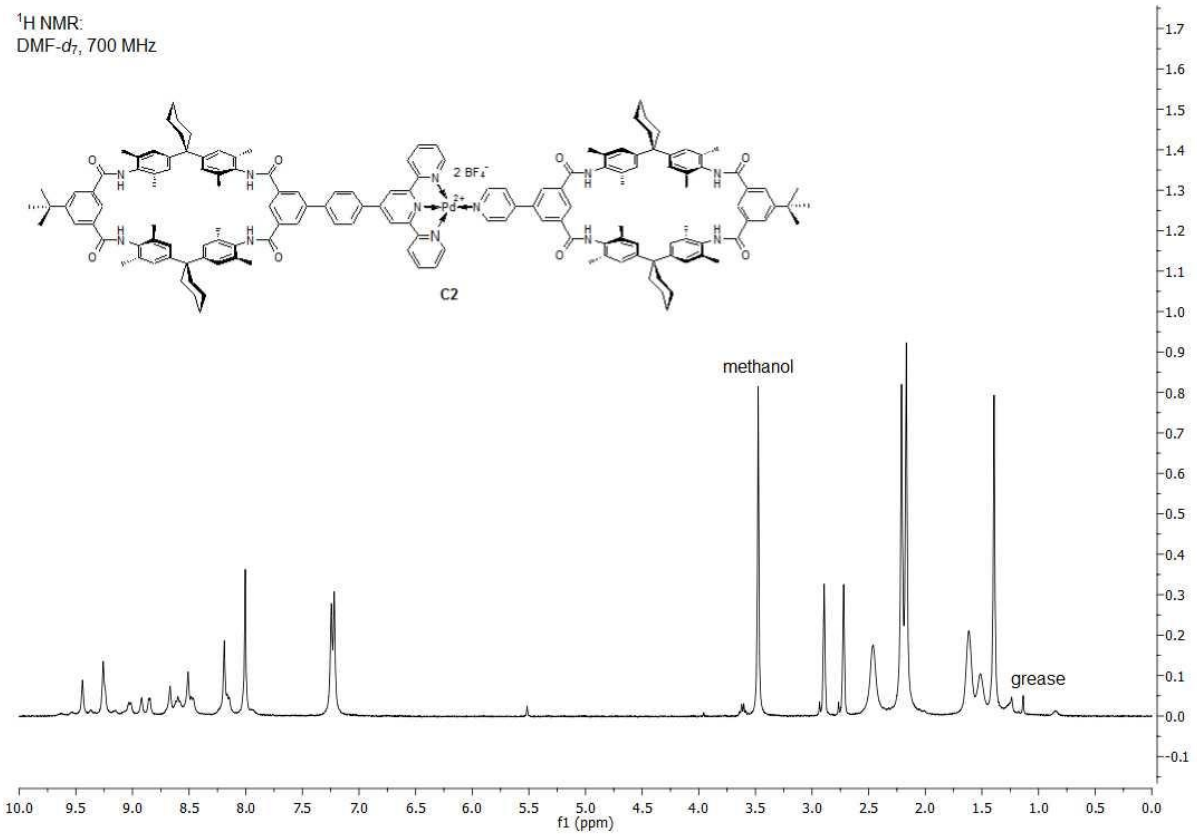

Figure S5: ^{1}H NMR spectrum of **tBuTMC-tBuPMC-Pd**.

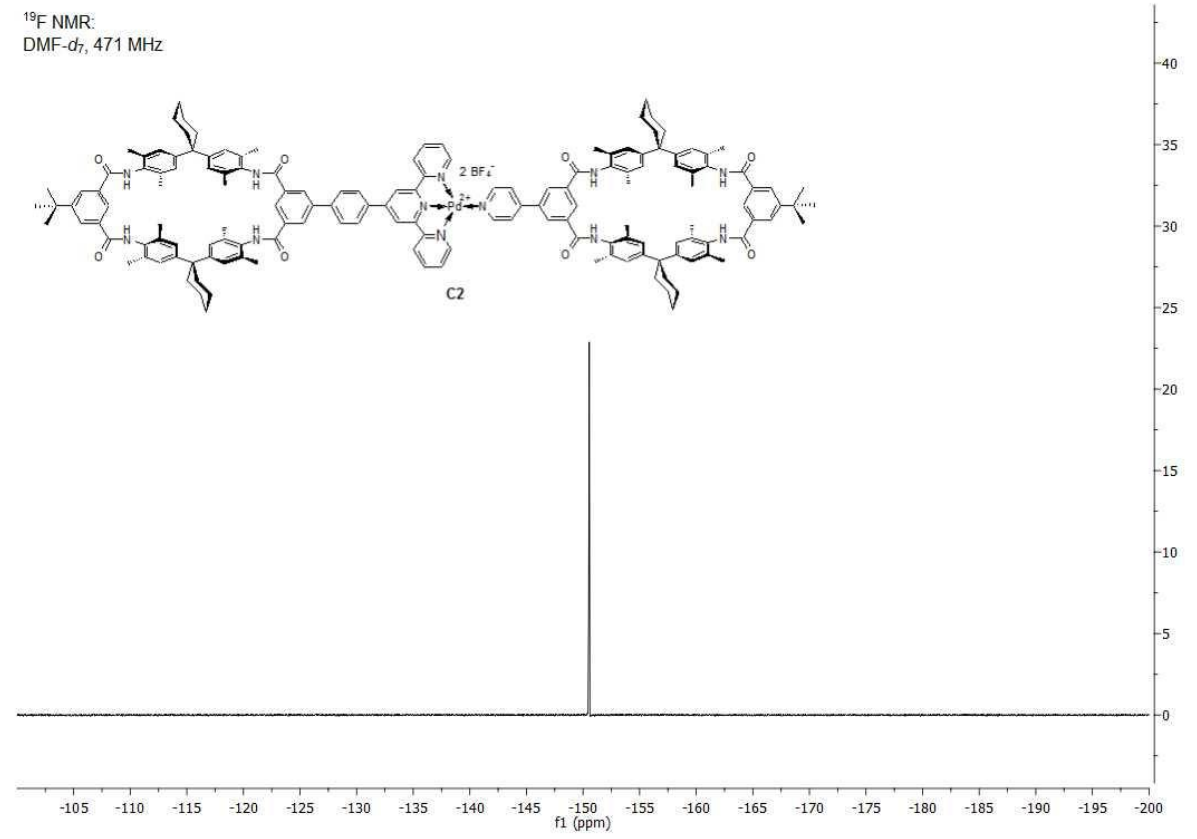

Figure S6: ^{19}F NMR spectrum of **tBuTMC-tBuPMC-Pd**.

6. Additional transmission-UV/Vis spectra

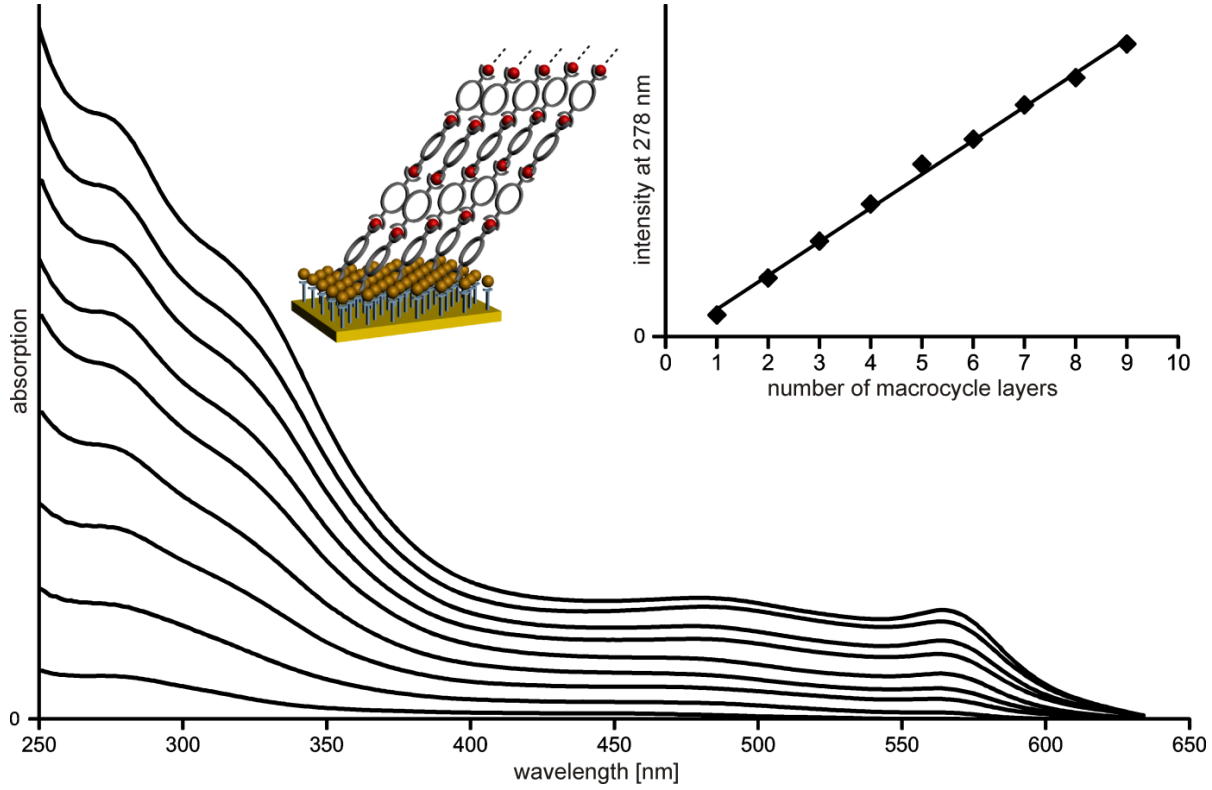

Figure S7: Transmission UV/Vis spectra of successful multilayer formation with **TMC** and Pd(II)/Fe(II) ions up to nine macrocycles, recorded after each macrocycle deposition step.

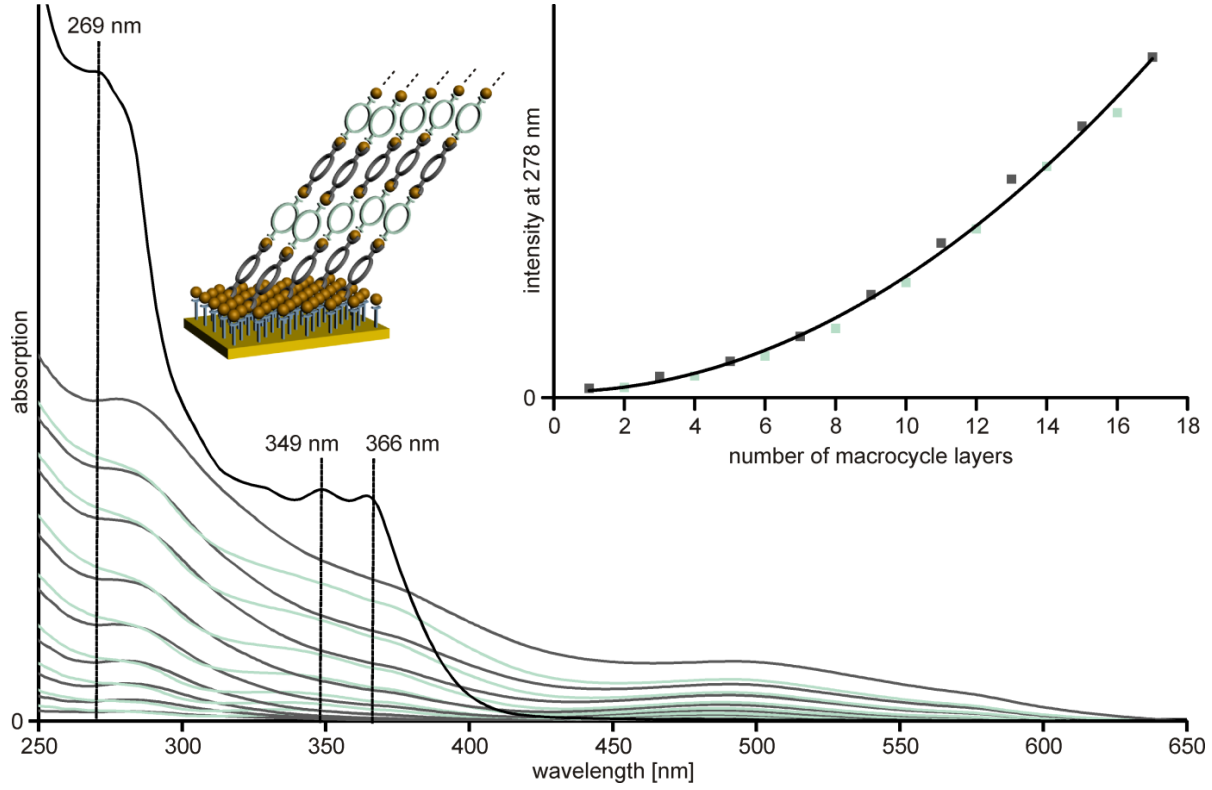

Figure S8: Transmission UV/Vis spectra of successful multilayer formation with **TMC**, **PMC** and Pd(II) ions up to seventeen macrocycles, recorded after each macrocycle deposition step (dark grey after **TMC** and light grey after **PMC** deposition). The black UV/Vis spectrum is a solution spectrum of the macrocycle-palladium complex **tBuTMC-tBuPMC-Pd**.

7. Additional XPS and NEXAFS data

Additional XPS data for a PMC Multilayer with *trans*-$PdCl_2$

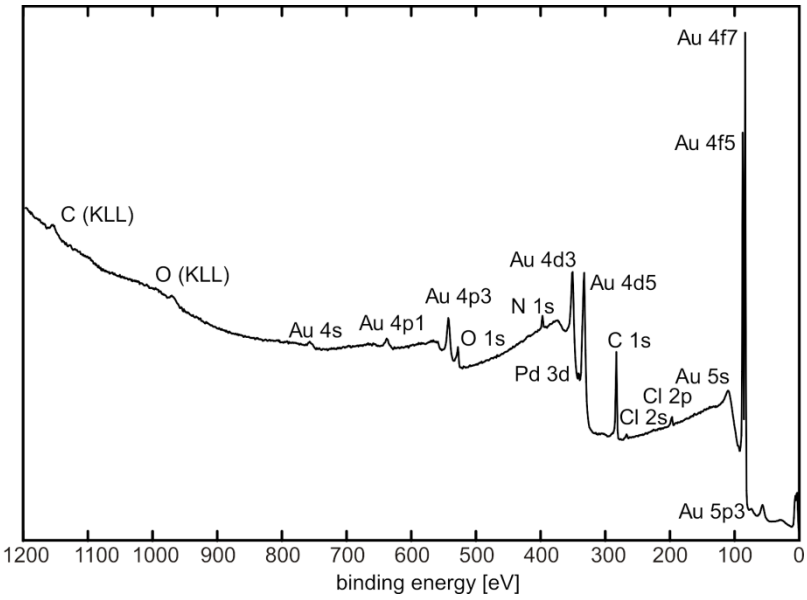

Figure S9: Survey XP spectrum of **PST**-SAM→(*trans*-$PdCl_2$→**PMC**)$_2$→*trans*-$PdCl_2$ on gold.

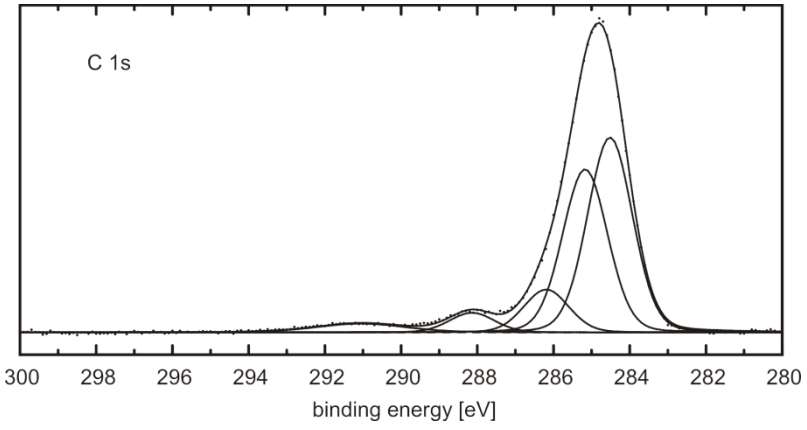

Figure S10: C 1s XP core level spectrum of **PST**-SAM→(*trans*-$PdCl_2$→**PMC**)$_2$→*trans*-$PdCl_2$ on gold.

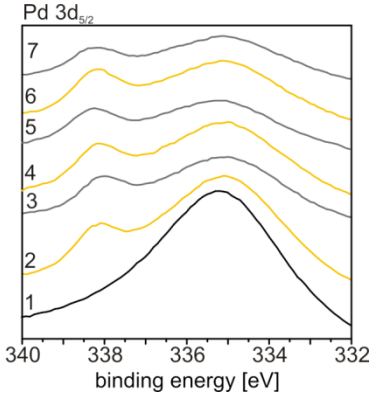

Figure S11: Pd $3d_{5/2}$ XP core level spectra of a multilayer of **PMC** and *trans*-$PdCl_2$ on **PST**. The spectra were recorded after each deposition step.

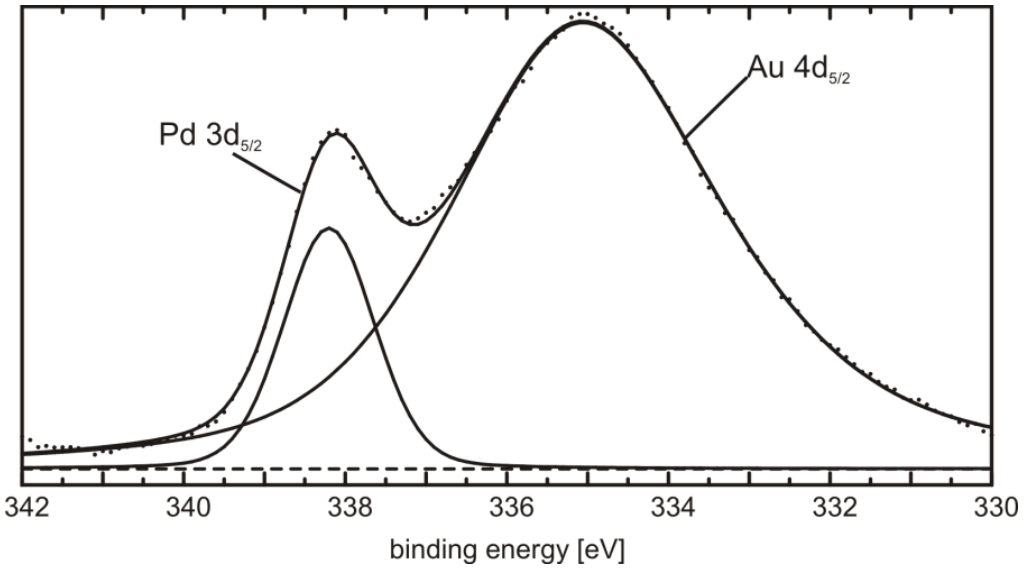

Figure S12: Peak fit of the Pd $3d_{5/2}$ XPS signal of **PST**-SAM→(*trans*-$PdCl_2$→**PMC**)$_2$→*trans*-$PdCl_2$ on gold.

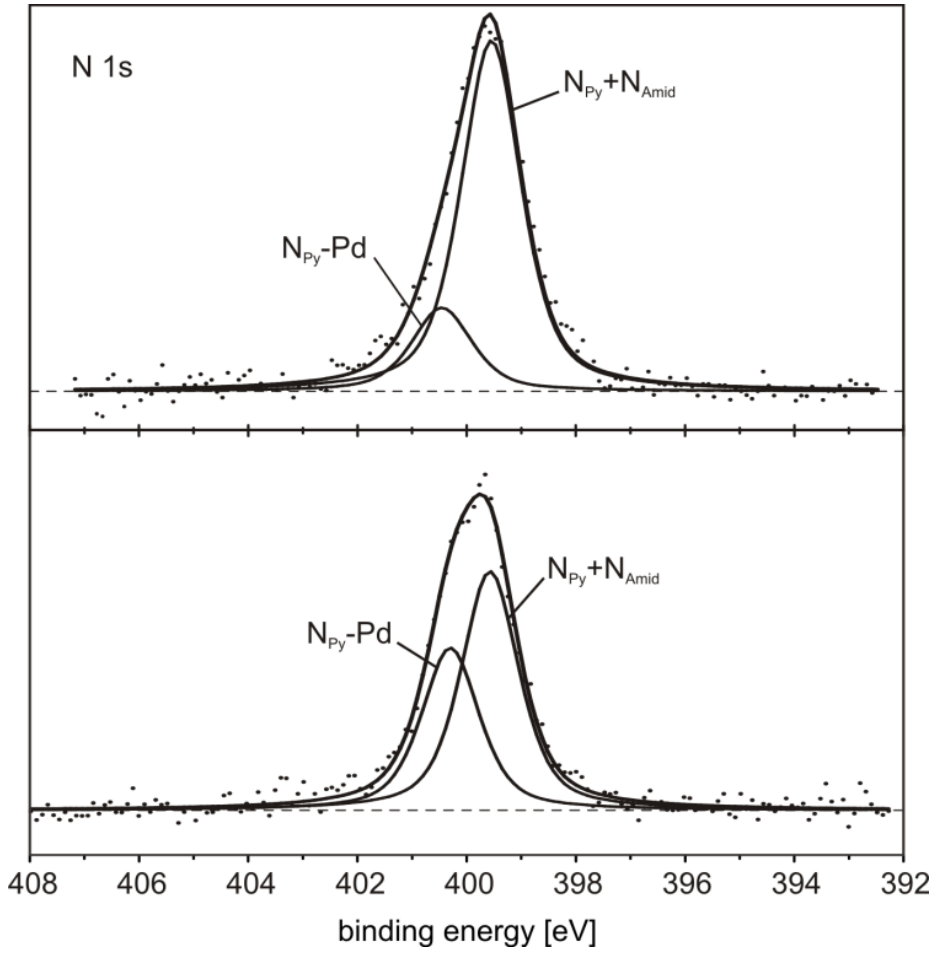

Figure S13: N 1s XP core level spectra of **PST**-SAM→(*trans*-$PdCl_2$→**PMC**)$_2$ (top) and **PST**-SAM→(*trans*-$PdCl_2$→**PMC**)$_2$→*trans*-$PdCl_2$ (bottom). The component at higher BE 400.7 eV can be assigned to complexed pyridine whereas the component at 399.8 eV is assigned to non-complexed pyridine and amide nitrogens.[5,7]

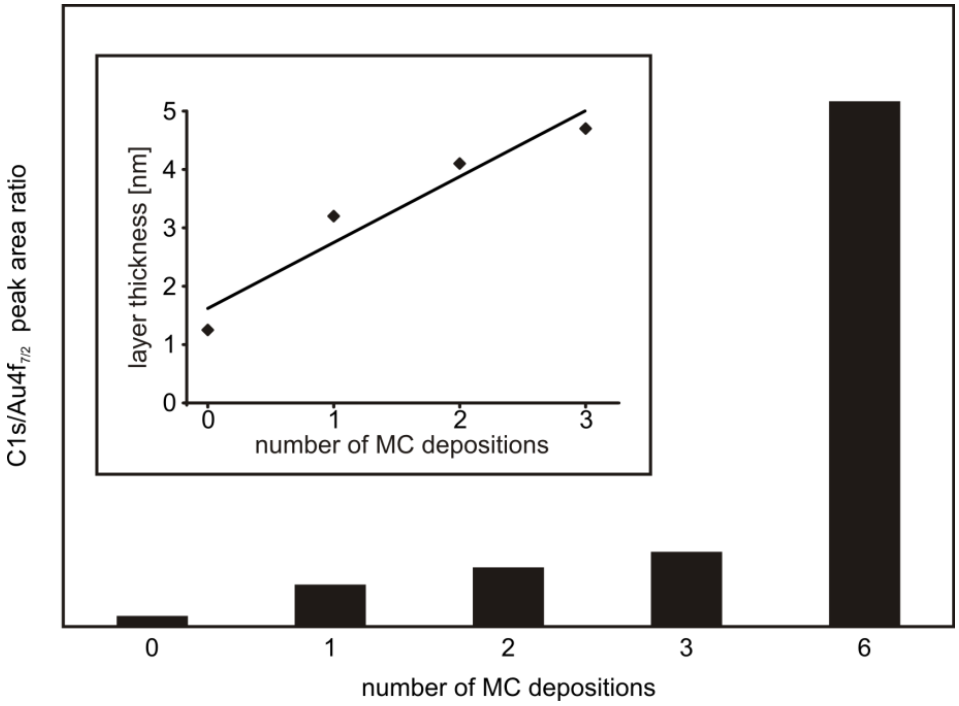

Figure S14: C 1s/Au 4f XPS peak area ratios of a **PMC** and *trans*-$PdCl_2$ multilayer on **PST** (60° emission angle) and the calculated layer thicknesses (inset).

Additional XPS and NEXAFS data for a mixed Multilayer of PMC, TMC, Pd(II), *trans*-$PdCl_2$, Fe(II) and Ni(II)

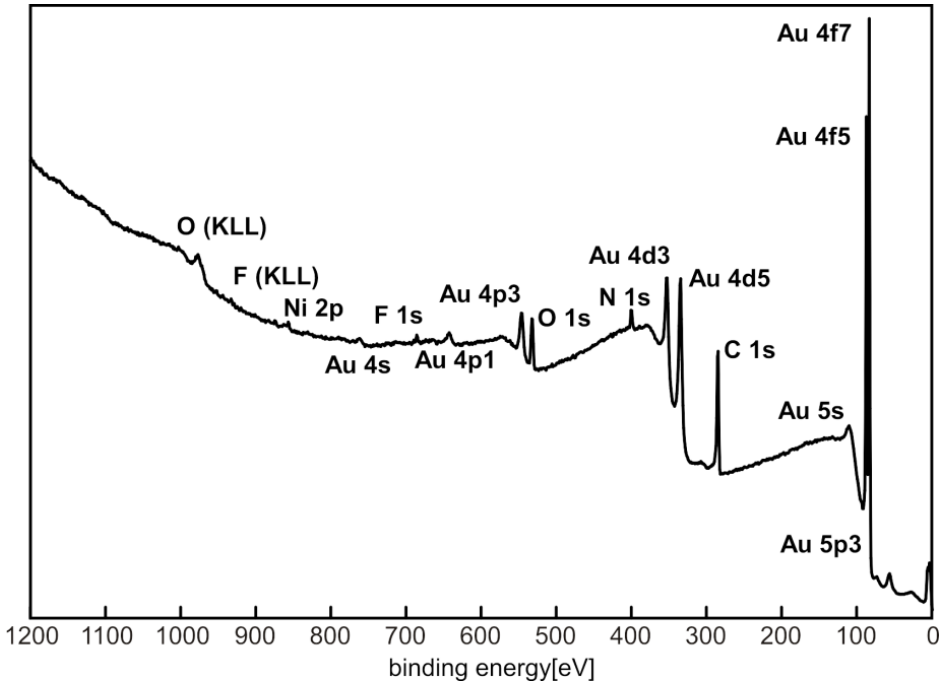

Figure S15: Survey XP spectrum of a **PST**-SAM→Pd(II)→**TMC**→Fe(II)→**TMC**→Pd(II)→**PMC**→*trans*-$PdCl_2$→**PMC**→Pd(II)→**TMC**→Ni(II) on gold.

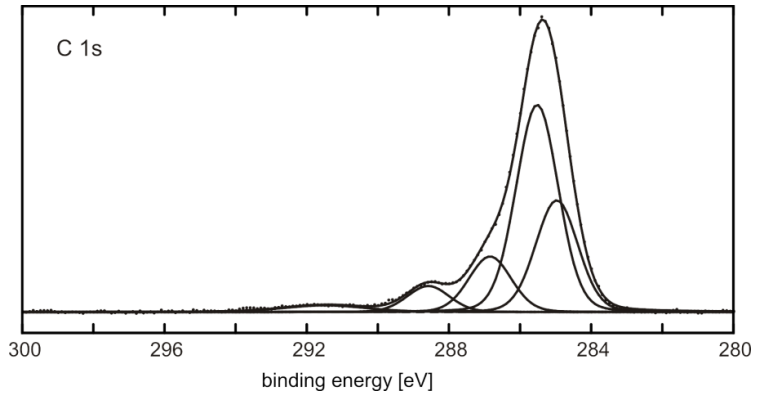

Figure S16: C 1s XP core level spectrum of **PST**-SAM→Pd(II)→**TMC**→Fe(II)→**TMC**→Pd(II)→**PMC**→*trans*-$PdCl_2$→**PMC**→Pd(II)→**TMC**→Ni(II) on gold.

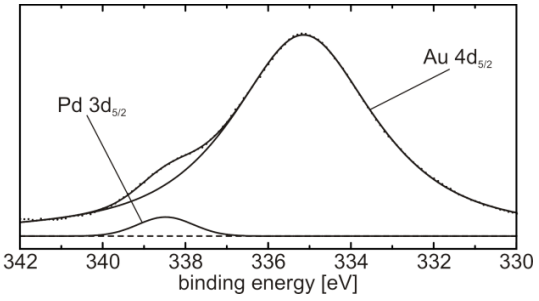

Figure S17: Peak fit of the Pd $3d_{5/2}$ XP spectrum of **PST**-SAM→Pd(II)→**TMC**→Fe(II)→**TMC**→Pd(II)→**PMC**→*trans*-$PdCl_2$ on gold.

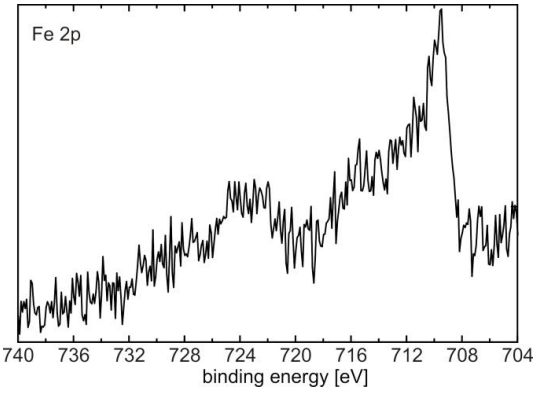

Figure S18: Fe 2p XP core level spectrum of **PST**-SAM→Pd(II)→**TMC**→Fe(II) on gold.

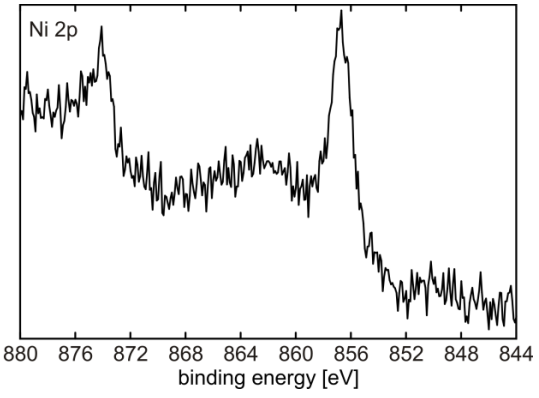

Figure S19: Ni 2p core level XP spectrum of **PST**-SAM→Pd(II)→**TMC**→Fe(II)→**TMC**→Pd(II)→**PMC**→*trans*-$PdCl_2$→**PMC**→Pd(II)→**TMC**→Ni(II) on gold.

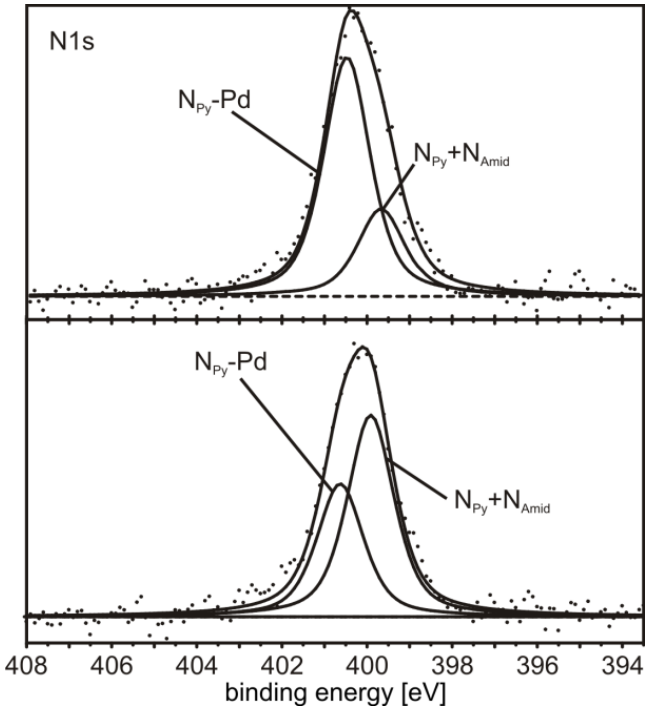

Figure S20: N 1s XP core level spectra of **PST**-SAM→Pd(II)→**TMC**→Fe(II)→**TMC**→Pd(II)→**PMC**→*trans*-$PdCl_2$ (top) and **PST**-SAM→Pd(II)→**TMC**→Fe(II)→**TMC**→Pd(II)→**PMC**→*trans*-$PdCl_2$→**PMC** (bottom). The component at higher BE 400.7 eV is assigned to complexed pyridine and terpyridine whereas the component at 399.8 eV is assigned to non-complexed pyridine and terpyridine and amide nitrogen.[5,7]

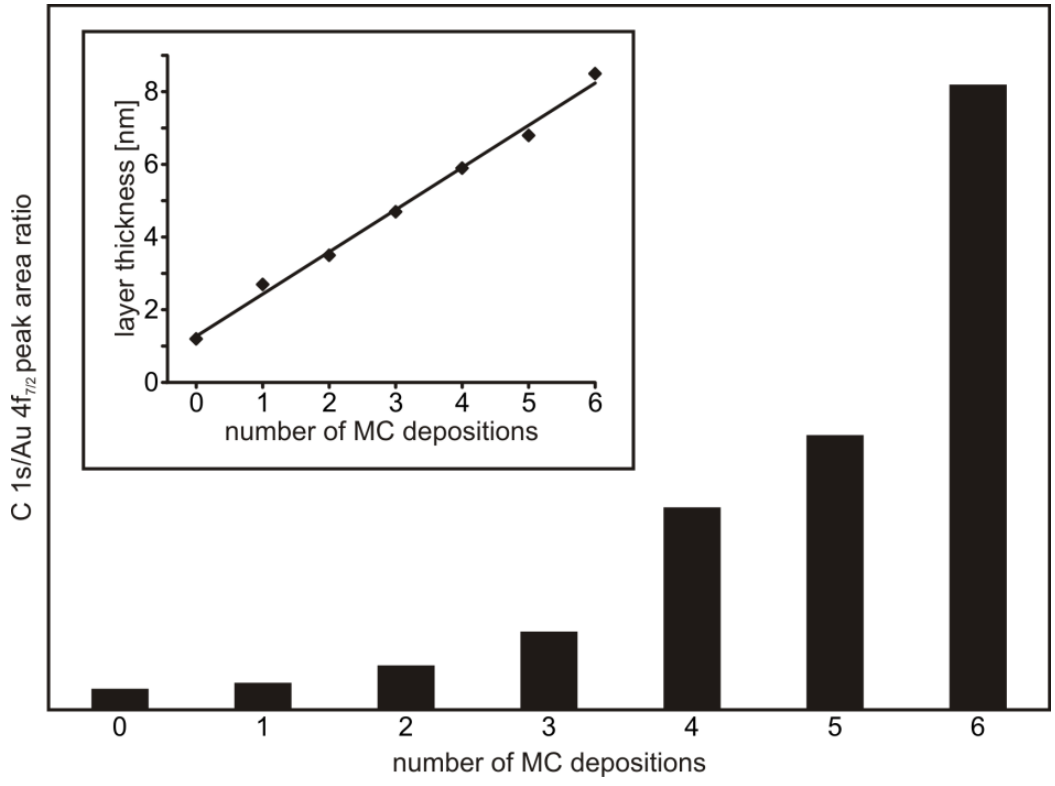

Figure S21: C 1s/Au 4f XPS peak area ratios of a mixed multilayer of **PMC**, **TMC**, Pd(II), *trans*-$PdCl_2$, Fe(II) and Ni(II) (60° emission angle) and the calculated layer thicknesses (inset).

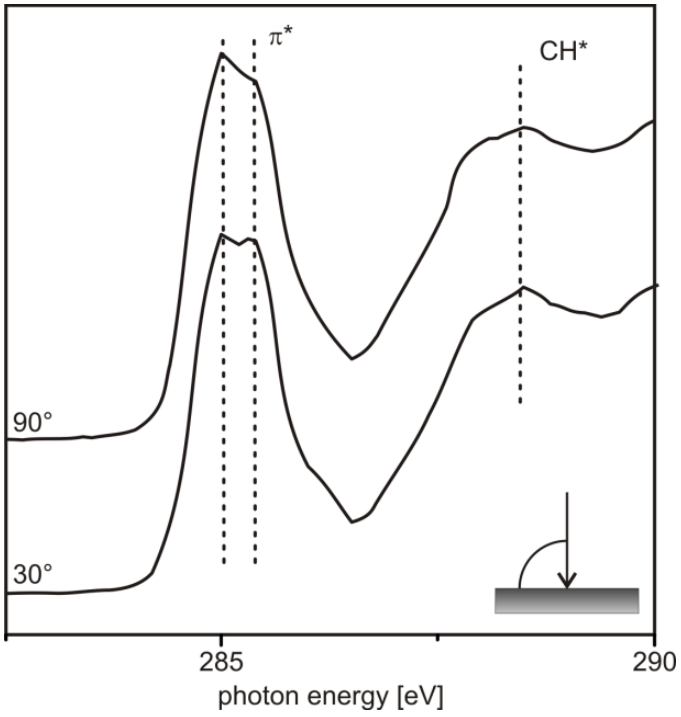

Figure S22: Angle-dependent C K-edge NEXAFS of **PST**-SAM→Pd(II)→**TMC**→Fe(II)→**TMC**→Pd(II)→**PMC**→*trans*-$PdCl_2$→**PMC**→Pd(II)→**TMC**→Ni(II)→**TMC** on gold**.**

8. References

1 S. V. Merzlikin, N. N. Tolkachev, T. Strunskus, G. Witte, T. Glogowski, C. Wöll and W. Grünert, *Surface Science,* 2008, **602**, 755-767.

2 M. P. Seah and W. A. Dench, *Surface and Interface Analysis,* 1979, **1**, 2-11.

3 J. Stöhr *NEXAFS Spectroscopy*; Springer, Heidelberg, Germany, 1992.

4 P. E. Batson, *Phys. Rev. Lett.,* 1982, **49**, 936-940.

5 J. Poppenberg, S. Richter, C. H.-H. Traulsen, E. Darlatt, B. Baytekin, T. Heinrich, P. M. Deutinger, K. Huth, W. E. S. Unger and C. A. Schalley, *Chem. Sci.,* 2013, DOI: 10.1039/C1033SC50558H

6 B. Baytekin, S. S. Zhu, B. Brusilowskij, J. Illigen, J. Ranta, J. Huuskonen, L. Russo, K. Rissanen, L. Kaufmann and C. A. Schalley, *Chem. Eur. J.,* 2008, **14**, 10012-10028.

7 S. Richter, J. Poppenberg, C. H. H. Traulsen, E. Darlatt, A. Sokolowski, D. Sattler, W. E. S. Unger and C. A. Schalley, *J. Am. Chem. Soc.,* 2012, **134**, 16289-16297.